Journal of Molecular Liquids 315 (2020) 113770

Contents lists available at ScienceDirect

Journal of Molecular Liquids

journal homepage: www.elsevier.com/locate/molliq

Synthesis and property of alkyl dioxyethyl α-*D*-xyloside

Xiubing Wu, Na Kuang, Langqiu Chen *, Yulin Fan, Fang Fu, Jiping Li, Jing Zhang

College of Chemistry, Key Laboratory of Environmentally Friendly Chemistry and Application of Ministry of Education, Xiangtan University, Xiangtan City, 411105, Hunan, People's Republic of China

ARTICLE INFO

Article history:
Received 2 May 2020
Received in revised form 1 July 2020
Accepted 6 July 2020
Available online 08 July 2020

Keywords:
Sugar-based surfactants
Alkyl dioxyethyl α-*D*-xyloside
Synthesis
Water solubility
Surface activity

ABSTRACT

Due to the inherent defects of the long alkyl chain in the related hydrophilicity and water solubility, alkyl α-*D*-xylosides (**7**) had hardly the practical application as sugar-based surfactants and should be reconstructed to obtain alkyl dioxyethyl α-*D*-xylosides (**5**) with dioxyethylene fragment (−(OCH_2CH_2)$_2$-)) as the hydrophilic spacer to increase the related *TPSA* value. With *D*-xylose as the raw material, 1,2-cis alkyl dioxyethyl α-*D*-xylosides (**5a-5f**, n = 6–12) were stereoselectively synthesized. Their physicochemical properties including water solubility, surface tension, foamability, emulsification, thermotropic liquid crystal, and hygroscopicity had been investigated. Their water solubility was found to decrease gradually whereas their calculated *HLB* numbers were 14.72 → 11.67 (n = 6 → 12) with increasing alkyl chain length (n). Dodecyl dioxyethyl α-*D*-xyloside (**5f**) had not water solubility because the *HLB* number was low. Furthermore, their *CMC* values decreased with increasing the alkyl chain length, and the *CMC* value of decyl dioxyethyl α-*D*-xyloside (**5e**) was as low as 9.21×10^{-5} mol·L^{-1}. Octyl dioxyethyl α-*D*-xyloside (**5c**) had the lowest surface tension (27.25 mN·m^{-1}) at the *CMC*. Both of nonyl and decyl dioxyethyl α-*D*-xylosides (**5d** & **5e**) possessed good foaming power and foam stability. Decyl dioxyethyl α-*D*-xyloside (**5e**) had the strongest emulsifying property either in the toluene/water system or in the octane/water system. Nonyl dioxyethyl α-*D*-xylosides (**5d**) had the most stylish S_A texture. Hexyl dioxyethyl α-*D*-xyloside (**5a**) possessed the strongest hygroscopicity. Therefore, the alkyl dioxyethyl α-*D*-xylosides as a class of novel sugar-based surfactants will be widely considered as promising candidates for various practical applications.

1. Introduction

For the fatty alcohol polyoxyethylene ethers (AEO) and the related derivatives, such as fatty alcohol polyoxyethylene ether carboxylate (AEC), sulfonate and sulfate, these surfactants have good biodegradability, water-solubility, salt tolerance, resistance to hard water, wetting ability, emulsifying capacity, foaming ability, detergency performance, lubrication, and flotation behavior, so they should have application value to a certain extent [1–4]. For example, AEO with a rather flexible hydrophilic part, as the conventional poly(ethylene oxide) (PEO)-based surfactants, can adsorb strongly on silica/water and air/water interfaces with the hydrogen bonding as the main driving force for the adsorption [3,4]. However, one may perceive an issue that the raw material ethylene oxide (EO) and its derivatives could be prepared from petroleum oil [5]. Due to a lot of unexpected events including the subprime mortgage crisis in 2007 and the current COVID-19 (the Corona Virus Disease 2019) pandemic, the relevant global economy should be seriously dragged down, resulting in a short-term downward tendency on oil prices [6,7]. Nevertheless, the petroleum oil, as a scarce fuel and non-renewable chemical raw materials, should be replaced to afford other valuable surfactants by some renewable resources to relieve/delay the energy crisis/depletion to certain content. Therefore, to avoid such an obstacle, much attention should be paid to the efficient synthesis of the related surfactants rather than petroleum-based surfactants.

On the contrary, carbohydrates should be attractive bioorganic materials on the earth because they are natural sources, environmentally friendly, and highly functionalized, thus promoting green and sustainable development in chemistry, life science, and functional materials [3,8]. Besides, sugar-based surfactants would indeed be available for various potential applications such as the chemical cleaning [9], the flotation [10], the oil recovery [11,12], the oil spill treatment [13], the textile printing and dyeing [14], the pesticides [15], the liquid crystal materials [16–19], the nanotechnology [20], the emulsion [21], the membrane protein research [22–25], the chemical catalysis [26], the pharmacology [27–31], the bacterial ecology [32], the toxicology [33], the antibacterial activity [34,35], the cosmetics [36], and biotechnology [37] due to their excellent surface activity, fine and stable foam, good biocompatibility, low/non-toxic, seldom irritation, easy biodegradation, and strong detergency. Also, such sugar-based surfactants would rather stay in the aqueous phase than adsorb on silica [3,4].

Besides polyethyleneglycol monoalkyl ether (C_nE_n) [38], alkyl glycosides such as alkyl xylosides [32], alkyl polyglucosides (APG) [39], alkyl β-*D*-maltoside [38], and NBD-alkyl lactosides [40], are classic nonionic

* Corresponding author.
E-mail address: chengood2003@263.net (L. Chen).

https://doi.org/10.1016/j.molliq.2020.113770
0167-7322/

surfactants. Because of the unique function of hydrophilic glycosyl group, the aqueous solutions of the sugar-based surfactants are less temperature-sensitive than those of alkyl polyoxyethylene ether solutions although the relevant water solubility decreases continuously with the extension of hydrophobic chain length, and such results should hint that the corresponding glycosides would be more advantageous than the corresponding non-ionic alkyl polyoxyethylene ethers in certain fields of application. Unlike alkyl polyoxyethylene ethers and polysorbates surfactants, alkyl glycosides surfactants such as dodecyl maltoside can be prepared as pure single-chemical species, so that it should be escaped from the serious issue of the mixtures with the various activity and more or less side products and even residual starting material. Furthermore, alkyl glycosides should be difficult to subject to oxidative degradation so that the related harmful immune response would be not elicited. Therefore, they can offer a potential alternative in the related therapeutic formulations, whether oral, nasal, anal and external use or injection [41].

However, for both complex APG and anomerically pure alkyl glycosides with long hydrophobic chains, their water solubility should be poor since their hydrophilicity should be low [42,43]. In this context, their applications would also be restricted to some content because of their low or no water solubility. Therefore, it would be eager to develop new surfactants with proper water solubility and excellent surface activity with long hydrophobic chains.

To the best of our knowledge, *D*-xylose should be the second most abundant monosaccharide with a reasonable low price after glucose because its natural polymer xylan is a renewable heterogeneous polysaccharide existing in the plant cell wall, accounting for about 15–35% of the dry weight of plant cells. As a major component of plant hemicellulose and a complex polypentacarbose, *D*-xylose can be easily obtained from the agricultural wastes and other biomass such as corn spike, bagasse wheat bran, and straw [37,43–45]. Thereof, we should make full of xylan, xylooligosaccharides and xylose to convert various value-added materials including xylitol, succinic acid, furfural, calorie-free sweetener, baked products, functional food (for the growth of probiotic Bifidobacterium), high-grade soy sauce color, pharmaceutical excipients, drug, chiral molecules, alkyl xylosides, and other products [32,43,46–50].

However, compared with other alkyl monoglycosides, alkyl xylosides should not be suitable for hydrophilic surfactants since they were not water solubility with longer alkyl chain (n) due to their small hydrophilic sugar portion. For the hexoses such as glucose and galactose, they have a strong hydrophilic hydroxymethyl group, but xylose lacks such group so that xylose's derivatives alkyl xylosides had the low water solubility and were even insoluble in water for the slight long alkyl chain [32,43]. Thus, the application of alkyl xylosides as surfactants would be severely limited. To make full use of the renewable and economical *D*-xylose from the agricultural waste, how to solve the water solubility barrier of its derivatives alkyl xylosides as a valuable surfactant is likely to be a key issue in the sustainable and environmentally friendly development process.

As shown in Fig. 1, in order to improve further the corresponding hydrophilicity and water solubility of alkyl α-*D*-xylosides (**7**), we attempt to introduce dioxyethylene fragment ($-(OCH_2CH_2)_2-$) as a hydrophilic spacer to prepare alkyl dioxyethyl α-*D*-xylosides (**5**) with *D*-xylose as raw material [42,51–53]. Their properties including *HLB* number, water-solubility, surface tension, foamability, emulsification, thermotropic liquid crystal, and hygroscopicity would be investigated as well, and the relationship between their structure and properties would be further disclosed. The data should provide a theoretical basis for their practical application value and market potential as the nonionic sugar-based surfactants.

2. Experimental

2.1. Material and instrument

Surface tension was measured with a BZY-2 full-automatic surface/interfacial tensiometer employing the Wilhelmy plate method (Shanghai Hengping Instrument and Meter Factory, China). Differential scanning calorimetry (DSC, TA-Q10, TA Instruments) was used for tracking the thermal transitions of the samples through a heating and cooling procedure at a scanning rate of 5 °C·min^{-1} with nitrogen as sweeping fluid. Liquid crystal texture was carried out by polarized optical microscopy (POM, Leica DM-LM-P) equipped with a Leica heating stage (FP82HT), the samples were heated and cooled at 5 °C·min^{-1}. All chemical reagents were analytically pure or chemically pure.

2.2. Synthesis

As shown in Fig. 1, alkyl dioxyethyl α-*D*-xylosides (**5a-5f**) were readily prepared by the Helferich method through three-step reactions. First of all, with *D*-xylose (**1**) as raw material, acetylation was taken to afford 1,2,3,4-tetra-*O*-acetyl-*D*-xylopyranose (**2**) at the catalysis of anhydrous NaOAc. Next, alkyl dioxyethyl 2,3,4-tri-*O*-acetyl-α-*D*-xyloside (**4a-4f**) was stereoselectively synthesized by the coupling reaction of **2** and diethylene glycol monoether (**3a-3f**) with $SnCl_4$ as the Lewis acid catalyst. Finally, alkyl dioxyethyl α-*D*-xyloside (**5a-5f**) was prepared through the deacetylated process of **4a-4f**. The detailed preparation and structural characterization were documented in the Support Information (SI).

3. Property

3.1. Hydrophilic-lipophilic balance (HLB) number and octanol-water partition coefficients (LogP) value

The *HLB* numbers of alkyl dioxyethyl α-*D*-xylosides (**5a-5f**) were calculated from Eq. (1) by the Griffin method [53–55].

$$HLB = \frac{20X}{W} \tag{1}$$

where *X* and *W* were the molecular mass of the hydrophilic portion and the whole molecular mass, respectively.

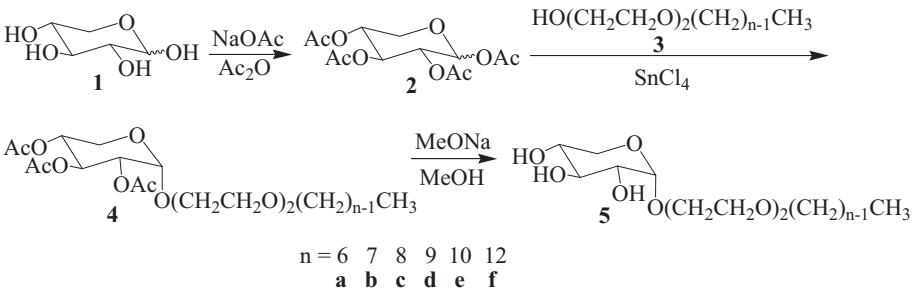

Fig. 1. Synthesis of alkyl dioxyethyl α-*D*-xylosides (**5a-5f**).

The Log*P* value of the synthetic alkyl dioxyethyl *α-D*-xyloside (**5a-5f**) was calculated by using ChemBioDraw (Ultra 14.0) to estimate their lipophilic character [53].

3.2. Solubility

The solubility of alkyl dioxyethyl *α-D*-xyloside (**5a-5f**) in water or ethanol was determined at room temperature (25 °C) with the described methods [52].

3.3. Surface tension

The surface tensions were measured at room temperature (25 °C) by using the BZY-2 full-automatic surface/interfacial tensiometer that was calibrated by double-distilled water. The aqueous solutions of alkyl dioxyethyl *α-D*-xylosides (**5a-5e**) were freshly prepared as a stock solution and then diluted to the desired concentration for each measurement. The Wilhelmy plate was rinsed with water, then flamed, whereas the glassware was rinsed with water and washed once with the sample solution to be tested before testing. The surface tension was measured three times for each concentration to reduce the measurement error.

The critical micelle concentration (*CMC*) and the surface tension at the *CMC* were determined from the breakpoint of the plot of the surface tension concerning the logarithm of the concentration. The relevant surfactant surface excess concentration at the air-solution interface (Γ_{max}) was calculated out by using the Gibbs adsorption isotherm equation (Eq. (2)) [52,56].

$$\Gamma_{max} = -\frac{1}{2.303\ nRT}\cdot\frac{d\gamma}{d\ \log C} \tag{2}$$

where γ *was* the surface tension, *C* was the surfactant concentration, *T* was the thermodynamic temperature (K), *R* represents the gas constant (8.314 $J\cdot mol^{-1}\cdot K^{-1}$), herein, n = 1 because alkyl dioxyethyl *α-D*-xylosides should be classified as a nonionic surfactant, and $d\gamma/d\log C$ was the slope below *CMC* in the surface tension plots. The area occupied by the surfactant molecule at the air-solution interface (A_{min}) was calculated by Eq. (3).

$$A_{min} = \frac{1}{N_A\Gamma_{max}} \tag{3}$$

where N_A is Avogadro's number (6.02×10^{23}). Besides, the effectiveness of reducing surface tension (π_{CMC}) was obtained by Eq. (4). The adsorption efficiency of reducing surface tension (pC_{20}) was calculated by Eq. (5) [52].

$$\pi_{CMC} = \gamma_0 - \gamma_{CMC} \tag{4}$$

$$pC_{20} = -\ \lg C_{20} \tag{5}$$

Herein, γ_0 represented the surface tension of the distilled water, γ_{CMC} was the surface tension of the aqueous solution at the *CMC*. C_{20} was the surfactant concentration required to reduce the surface tension by 20 $mN\cdot m^{-1}$.

The standard free energy of micellization (ΔG_{mic}) and surface adsorption free energy (ΔG_{ads}) for the nonionic surfactants were calculated using the relevant equations (Eqs. (6) and (7)) [52,57].

$$\Delta G_{mic} = RT\ \ln(\mathrm{CMC}) \tag{6}$$

$$\Delta G_{ads} = \Delta G_{mic} - \pi_{CMC}/\Gamma_{max} \tag{7}$$

3.4. Foaming property

According to the literature [52,53], the foaming property of the aqueous solution of alkyl dioxyethyl *α-D*-xylosides (**5a-5e**) was determined at 25 °C. An aqueous solution of alkyl dioxyethyl *α-D*-xylosides (0.25% (w/w)) 10 mL was obtained and transferred to a 100-mL graduated cylinder with a plug. The initial volume of foam (V_0) was recorded just after 60 s of intense shock, which evaluating the foaming performance according to the initial volume of foam. Just after the solution kept in a static state for 5 min, the foam volume (V_5) was recorded, the foam stability was evaluated by Eq. (8) according to the foam disappearance rate (υ).

$$\upsilon = \frac{V_0 - V_5}{t}\ (cm^3\ s^{-1}) \tag{8}$$

3.5. Emulsifying property

According to the literature [58], the emulsifying property of alkyl dioxyethyl *α-D*-xylosides (**5a-5e**) was measured at 25 °C. A series of aqueous surfactant solutions (0.25% (w/w)) were prepared. At first, a 20 mL aqueous solution of alkyl dioxyethyl *α-D*-xyloside was put into a 100-mL cylinder with a plug, and n-octane of 20 mL as the oil phase was added. The related mixture was strongly shocked for 60 s and kept in a static state for 1 h, and the volumes of the water layer, the emulsion layer, and the oil layer were recorded respectively. The emulsifying ability was determined according to the volume of the emulsion layer.

3.6. Thermotropic phase behavior

The thermal phase transition behavior of alkyl dioxyethyl *α-D*-xylosides was measured by polarizing optical microscopy (POM) during the heating and cooling process, and the rate of temperature change was controlled at 5 °C·min^{-1}. The phase transition temperature of alkyl dioxyethyl *α-D*-xylosides was observed by DSC [53].

3.7. Hygroscopicity

Approximately 1.00 g of each dried sample was placed in hermetic pots in the surround of the relative humidity (*RH* = 81% or 43%), the sample was weighed again after 2 h, 4 h, 6 h, 8 h, 12 h, 24 h, 48 h, 72 h, respectively. The hermetic pots were kept in an incubator with controlled temperature (25 °C). The hygroscopicity (***M***) of alkyl dioxyethyl *α-D*-xylosides was expressed by Eq. (9) [55].

$$M = \frac{M_t - M_0}{M_0}\times 100\% \tag{9}$$

where M_0 was the initial quality of samples, and M_t was the quality of samples after the test time.

4. Results and discussion

4.1. Preparation and structural characterization

In Fig. 1, with *D*-xylose (**1**) was used as the starting material, alkyl dioxyethyl *α-D*-xylosides (**5a-5f**) were readily prepared by a three-step reaction involving acetylation, stereoselective coupling with diethylene glycol monoether (**3a-3f**) and deacetylation. Herein, the Helfrich procedure was concisely used to get stereoselectively a series of protected *α-D*-xylosides (**4a-4f**). The corresponding chemical shift (δ) (coupling constant) of the anomeric hydrogen (H-1) in $CDCl_3$ was 5.06 ppm ($J_{1,2}$ = 3.6 Hz) (**4a**). The data disclosed that the coupled compound was 1,2-cis α-anomer [51,53]. The protected *α-D*-xylosides (**4a-4f**) were deacetylated to obtain alkyl dioxyethyl *α-D*-xylosides (**5a-5f**) which were 1,2-cis *α*-anomers by the NMR spectroscopy [51,59]. The preparation process and the NMR data were compiled in Supporting information (SI) in detail. Table 1 also showed that the chemical shifts (δ)

Table 1
Chemical shift (δ, ppm) ($J_{1,2}$, Hz) of alkyl dioxyethyl β-*D*-xyloside (**5a-5f**) in solvent.

Glycoside (n)	**a** (6)	**b** (7)	**c** (8)	**d** (9)	**e** (10)	**f** (**12**)
Chemical shift ($J_{1,2}$)	4.85 (3.7)	4.88 (3.6)	4.86 (3.6)	4.85 (3.6)	4.61 (3.7)	4.61 (3.6)
solvent	D_2O	D_2O	D_2O	D_2O	DMSO-d_6	DMSO-d_6/D_2O

(the related coupling constants) of H-1 for the prepared 1,2-cis α-*D*-xylosides (**5a-5f**) were 4.61–4.88 ppm ($J_{1,2}$ = 3.6–3.7 Hz).

4.2. Hydrophilic characteristics

The *HLB* number is introduced to be convenient for the explanation of the functional properties of various surfactants. The high *HLB* number should be ascribed to the hydrophilic surfactants, which would be handily used to construct spontaneously the oil-in-water (O/W) micellar microstructure by supramolecular self-assembly. Whereas the lipophilic surfactants would be considered to possess low *HLB* number, they would be applied to stabilize spontaneously water-in-oil (W/O) emulsions. In this paper, the related *HLB* numbers of alkyl dioxyethyl α-*D*-xylosides (**5a-5f**) were calculated by the Griffin method, and the results were listed in Table 2 [53–55].

From Table 2, the *HLB* numbers of alkyl dioxyethyl α-*D*-xylosides (**5**) were from 14.72 (n = 6) to 11.67 (n = 12) with increasing alkyl chain length (n). By making a sharp contrast with alkyl α-*D*-xylosides (**7**), the *HLB* number of alkyl dioxyethyl α-*D*-xyloside (**5a-5f**) was bigger than the *HLB* number of alkyl α-*D*-xyloside (**7a-7f**) with the same alkyl chain length [53].

The logarithm of the partition coefficient between octanol-water (Log*P*) is often used to represent the molecular lipophilicity, which is an important parameter in many areas, including modeling pharmacological and toxicological properties, metabolism of molecules, the environmental fate of chemicals, aggregation of surfactants, detergency and coagulation. The Log*P* values of alkyl dioxyethyl α-*D*-xylosides (**5a-5f**) were calculated by ChemBioDraw (Ultra 14.0) to estimate their hydrophobicity [58].

From Table 2, the Log*P* values of alkyl dioxyethyl α-*D*-xylosides (**5**) were smaller than the Log*P* values of alkyl α-*D*-xylosides (**7**) with the same alkyl chain length. The data should be considered as reasonable and rather valuable since the dioxyethylene fragment as a hydrophilic group was introduced to enlarge from the xylosyloxy group ($C_5H_9O_5$-) of **7** to the xylosyloxyethyloxyethyloxy group ($C_5H_9O_5(CH_2CH_2O)_2$-) of **5** for the related hydrophilic partion, just as described in Fig. 2. Meanwhile, their topological polar surface areas (*TPSA*) were estimated as 97.61 Å^2 by ChemBioDraw (Ultra 14.0), obviously higher than the related TPSA (79.15 Å^2) of **7** or its anomer alkyl β-*D*-xylosides (**6**) [8,43]. Hence, their difference (97.61–79.15 = 18.46 Å^2) between **7** and **5** indeed responded to the hydrophilic impact due to the insertion of the hydrophilic heteroatoms (two oxygen atoms) with the hydrophilic spacer ($-(CH_2CH_2O)_2$-). At first, the related data of the *HLB* number, Log*P* value, and TPSA have used bioavailability screening and molecular modification of the huge druglike molecules, prodrugs, and other active molecules involving the molecular transport properties, particularly intestinal absorption, and blood-brain barrier (BBB) penetration. However, in the virtual sugar-based surfactant library, they should also be helpful in the respect of fast and effective screening of water solubility, surface activity, bioavailability, and other functionality.

Table 2
HLB numbers and Log*P* values of alkyl α-*D*-xylosides and alkyl dioxyethyl α-*D*-xylosides.

Alkyl α-*D*-xyloside (n)	Log*P*	*HLB*	Water solubility	Alkyl dioxyethyl α-*D*-xyloside (n)	Log*P*	*HLB*	Water solubility
7a (6)	0.60	12.73	Soluble	**5a** (6)	0.29	14.72	High
7b (7)	1.02	12.01	Soluble	**5b** (7)	0.70	14.10	High
7c (8)	1.43	11.37	Low	**5c** (8)	1.12	13.54	High
7d (9)	1.85	10.79	Low	**5d** (9)	1.54	13.02	Soluble
7e (10)	2.27	10.27	Insoluble	**5e** (10)	1.96	12.54	Soluble
7f (12)	3.10	9.37	Insoluble	**5f** (12)	2.79	11.67	Insoluble

The solubility of alkyl dioxyethyl α-*D*-xylosides (**5a-5f**) in water and ethanol at 25 °C was shown in Fig. 3. Their solubility in water and in ethanol decreased gradually with increasing alkyl chain length (n). The solubility in ethanol was bigger than that in water. Shorter alkyl chain α-*D*-xylosides (**5a-5e**, n = 6–10) were observed to have better water solubility. Among them, decyl dioxyethyl α-*D*-xyloside (**5e**) could still be dissolved in water with the water solubility of 41.8 g, and the related *HLB* number was 12.54, but dodecyl dioxyethyl α-*D*-xyloside (**5f**) was insoluble in water, and the related *HLB* number was 11.67, which was smaller than 12.00. Therefore, alkyl dioxyethyl α-*D*-xylosides were observed to have not water solubility with n ≥ 12, *HLB* ≤ 11.67, and Log*P* ≥2.79. For octyl/decyl/dodecyl α-*D*-glucopyranoside (**8c/8e/8f**), their *HLB* numbers, log*P* values, *TPSA* values and water-solubilities were 12.3/11.2/10.3, 0.90/1.73/2.57, 99.38/99.38/99.38 Å^2, and 0.51 g/0.06 g/insoluble, in respective. Whereas, for octyloxyethyl/decyloxyethyl/dodecyloxyethyl α-*D*-glucopyranoside (**9c/9e/9f**), their *HLB* numbers, Log*P* values, *TPSA* values and water solubilities were 13.3/12.2/11.4, 0.74/1.58/2.41, 108.61/108.61/108.61 Å^2, and 54.76/22.59/3.02 g, in respective. Hence, dodecyl dioxyethyl α-*D*-xylosides (**5f**) and dodecyl α-*D*-glucopyranoside (**8f**) had similar *TPST* values (97.61 and 99.38 Å^2), so that they were generally considered as insolubility in water.

As compared to the water solubility of alkyl α-*D*-xylosides (**7**), the water solubility of alkyl dioxyethyl α-*D*-xyloside (**5**) was much higher than alkyl α-*D*-xylosides (**7**) with the same alkyl chain length (n). The α-*D*-xylosides (**7**) with n ≥ 8 showed very low water solubility. Indeed, decyl α-*D*-xyloside (**7e**) was insoluble in water so that such alkyl α-*D*-xylosides (**7**) should be hardly found to have the practical application as hydrophilic sugar-based surfactants. Hence, it should be considered how to reconstruct the structure? It should be said that a rational methodology was used to improve the water solubility, i.e. dioxyethene fragment ($-(CH_2CH_2O)_2$-) as the hydrophilic spacer was inserted into between the xylosyl and alkyl group to enrich the hydrophilic partition and increase their *HLB* numbers and *TPSA* values. A series of novel compounds alkyl dioxyethyl α-*D*-xyloside (**5**) were prepared to solve successfully the issue. The experimental result has made an active reply.

The results revealed that the dioxyethylene segment indeed strengthened hydrophilicity and improved water solubility by enriching the intermolecular hydrogen-bond network. Besides, alkyl dioxyethyl α-*D*-xyloside with such hydrophilic fragment can broaden the application scope due to increasing the *TPSA* values (79.15 Å^2 → 97.61 Å^2) and improving the water solubility.

4.3. Interfacial property

The surface tension of different concentration of aqueous alkyl dioxyethyl α-*D*-xylosides (**5a-5e**) solution was measured by the BZY-2 full-automatic surface/interfacial tensiometer. However, the surface tension of dodecyl dioxyethyl α-*D*-xyloside (**5f**) was not investigated because of its insolubility in water.

Fig. 4 presented the relationship between the surface tension (γ) and the concentration (*C*). Increasing the alkyl chain length resulted in decreasing the critical micelle concentration (*CMC*). The surface tension value (γ_{CMC}) firstly decreased and then increased with increasing the alkyl chain length at the *CMC* although their difference was not very obvious, and octyl dioxyethyl α-*D*-xyloside (**5c**) possessed the lowest surface tension (27.26 mN·m^{-1}) at its *CMC*. Compared with some fundamental interfacial adsorption parameters of the traditional alkyl β-*D*-xylosides, the *CMC* values and γ_{CMC} values of the synthesized alkyl dioxyethyl α-*D*-xylosides were found to be less than that of alkyl *D*-xylosides [43]. The results indicated that introducing the

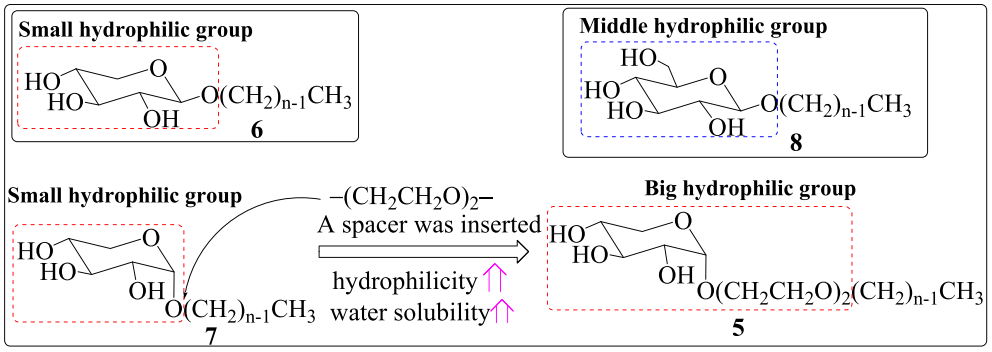

Fig. 2. The hydrophilic fragment is introduced to form alkyl dioxyethyl xyloside.

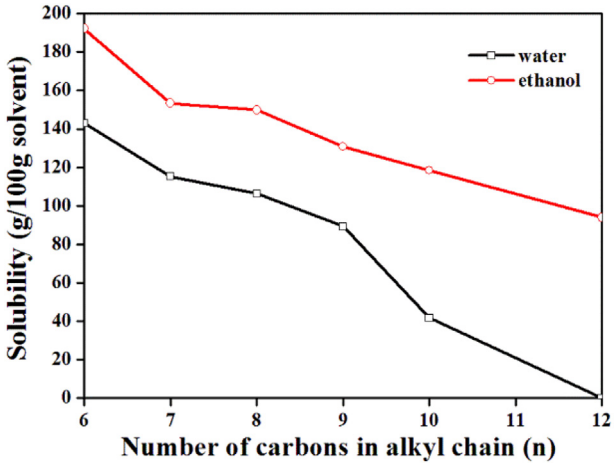

Fig. 3. The solubility of alkyl dioxyethyl *α-D*-xylosides in water or ethanol.

dioxyethylene fragment indeed improved the surface-active properties of glycosides to some extent.

Table 3 listed the *CMC*, Γ_{max}, and A_{min} values. First of all, the *CMC* values decreased gradually from 8.31×10^{-4} mol·L^{-1} (**5a**, n = 6) to 9.21×10^{-5} mol·L^{-1} (**5e**, n = 10). However, the γ_{CMC} values first decreased to the lowest, then increased with increasing the alkyl chain length, i.e. from 28.06 mN·m^{-1} (**5a**, n = 6) → 27.25 mN·m^{-1} (**5c**, n = 8) → 28.86 mN·m^{-1} (**5e**, n = 10). For the short alkyl chain, for example, hexyl dioxyethyl *α-D*-xyloside (**5a**), more free energy was required to form micelles and thereby resulting in a higher *CMC* value (8.31×10^{-4} mol·L^{-1}) due to its small hydrophobic group which would stretch out and had in contact with water to some content. Furthermore, the Γ_{max} values tended to increase from 4.93×10^{-6} mol·m^{-2} (**5a**, n = 6) to 6.64×10^{-6} mol·m^{-2} (**5e**, n = 10) with increasing the alkyl chain length. On the contrast with the Γ_{max} values, there can be no doubt that the A_{min} value showed a decreasing trend from 33.67 Å^2 (**5a**, n = 6) to 25.01 Å^2 (**5e**, n = 10) with increasing the alkyl chain length, which was just similar to the changing trend of the *CMC* value. Both of the Γ_{max} and the A_{min} values were a sign of the packing densities of the absorbed molecules at the air-solution interface. The larger Γ_{max} value and the smaller A_{min} value should correspond to the denser arrangement at the air-solution interface. It was disclosed that the molecular arrangement in longer alkyl chain *α-D*-xyloside was much denser than that in shorter alkyl chain *α-D*-xyloside. Because there should be the repulsive force between hydrophobic alkyl chain and water, the longer alkyl chain *α-D*-xyloside would readily adsorb onto the air-solution interface, such surfactant molecule would have the better ability to maintain less contact with water via the strong hydrophobic interaction between the long hydrocarbon chains [60,61].

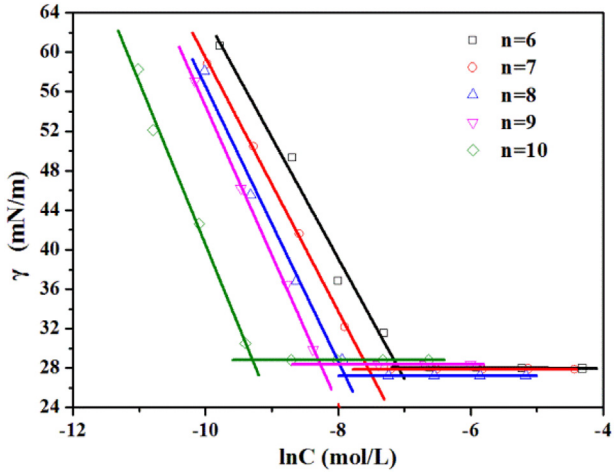

Fig. 4. The surface tension of alkyl dioxyethyl *α-D*-xyloside (**5a-5e**).

The obtained pC_{20} values showed an increasing trend with increasing the alkyl chain length, which indicated that decyl dioxyethyl *α-D*-xyloside (**5e**) had the highest adsorption efficiency, and the related tendency to adsorb at the air-water interface was the greatest. But, the obtained π_{CMC} values revealed that first increased rapidly, then decreased with increasing the alkyl chain length, i.e. from 43.91 mN·m^{-1} (**5a**, n = 6) → 44.72 mN·m^{-1} (**5c**, n = 8) → 43.11 mN·m^{-1} (**5e**, n = 10).

The standard free energy of micellization (ΔG_{mic}) was negative for the prepared sugar-based nonionic surfactants (**5a-5e**), suggesting that the micellization process was spontaneous. Whereas surface adsorption free energy (ΔG_{ads}) implied that the surfactants **5a-5e** had a great ability to adsorb at the air-water interface. With the same alkyl chain length, their negative ΔG_{mic} values were deduced to be smaller than their negative ΔG_{ads} values, indicating that the adsorption was promoted more than the micellization. Besides, both of negative ΔG_{mic} values and negative ΔG_{ads} values increased with increasing alkyl chain

Table 3
Interfacial property of alkyl dioxyethyl *α-D*-xyloside.

Alky dioxyl *α-D*-xylosides	5a	5b	5c	5d	5e
CMC ($\times 10^{-5}$ mol·L^{-1})	83.1	53.1	37.3	25.2	9.21
γ_{CMC} (mN·m^{-1})	28.06	27.89	27.25	28.70	28.86
Γ_{max} ($\times 10^{-6}$ mol·m^{-2})	4.93	5.18	5.61	6.08	6.64
A_{min} (Å^2)	33.67	32.08	29.61	27.31	25.01
pC_{20}	3.93	4.09	4.20	4.27	4.65
π_{CMC} (mN·m^{-1})	43.91	44.08	44.72	43.27	43.11
ΔG_{mic} (kJ·mol^{-1})	−17.58	−18.69	−19.57	−20.54	−23.04
ΔG_{ads} (kJ·mol^{-1})	−26.49	−27.21	27.54	−27.66	−29.53

length, suggesting that the driving force of the micellization and/or the adsorption was derived from the hydrophobic alkyl moieties due to the hydrophobic interaction between alkyl chains, those results were powerfully supported by the pC_{20} values, *HLB* numbers, and Log*P* values as described above [62].

4.4. Foaming property and emulsifying property

Generally speaking, the bigger the foaming volume (V_0), the better the foaming performance; the slower the foam disappearing rate (ν), the better the foam stability. In addition, the foaming ability and the foam stability probably were closely related to each other since the surfactant molecules would adsorb on the liquid film to form strong or weak adsorption film to stabilize the various foam.

Fig. 5 plotted the foaming property of alkyl dioxyethyl α-*D*-xylosides (**5a-5e**). The results showed that their foam volume (V_0) first increased significantly from the bottom to a high platform (62 mL, **5d** (n = 9)), and then decreased slightly with increasing the alkyl chain length. Among these glycosides, **5d** had the strongest foaming performance. Their foam disappearing rate (ν) gradually decreased from the high point to almost zero (**5a** → **5d** and **5e**) with increasing the alkyl chain length. Although the foam of **5a** vanished the fastest, **5d,** and **5e** were observed to have the minimum disappearance rate (υ = 0.01 mL·s^{-1}). Therefore, both of **5d** and **5e** were considered to have good foaming property and foam stability in such homologous series.

For an emulsion system, the hydrophilicity and hydrophobicity of an emulsifier would have an important impact on the type of the emulsified layer. In general, when the *HLB* number of a used emulsifier is 3.5–6, the related emulsified layer should be the W/O type; however, the related emulsified layer should be the O/W type when the *HLB* number of a used emulsifier is 8–18. For alkyl dioxyethyl α-*D*-xylosides (**5a** → **5e**), their calculated *HLB* numbers were 14.72 → 12.54 and their LogP values were 0.29 → 1.96 with increasing the alkyl chain length (n = 6 → 10). Therefore, their emulsified layer should reasonably be oil-in-water (O/W) either in the toluene/water system or in the n-octane/water system with the related concentration of 0.25%.

As shown in Fig. 6, the emulsifying ability in the n-octane/water system was, on the whole, stronger than that in the toluene/water system although both systems had rather near emulsion layer for **5a** (n = 6) with the short hydrophobic alkyl chain length. Their emulsion layers thickened monotonously with increasing the alkyl chain length, **5e** (n = 10) had the best emulsifying ability in both systems. A shorter hydrophobic chain in such sugar-based surfactants would severely hinder the hydrophobic interactions between the surfactant and the oil phase at the interface at all, which further weakened the adsorption at the interface. On the contrary, a longer hydrophobic chain made the α-*D*-xyloside itself migrated more easily away from the bulk solution and went onto the interface to form readily a stronger interfacial film, preventing the discontinuous liquid particles of the dispersed phase in the emulsion layer from reaggregation [63]. However, the emulsifying ability would not keep strengthening with increasing the alkyl chain length because not only the appropriate *HLB* number, and Log*P* value but also the rational *TPAS* value, and water solubility should be demanded to certain content. Excessive long hydrophobic alkyl chain made the related *HLB* number too small and Log*P* value too big with the same *TPAS* value, which would destroy the hydrophilic and hydrophobic balance in the O/W emulsion due to violating of the Bancroft rule [64–66].

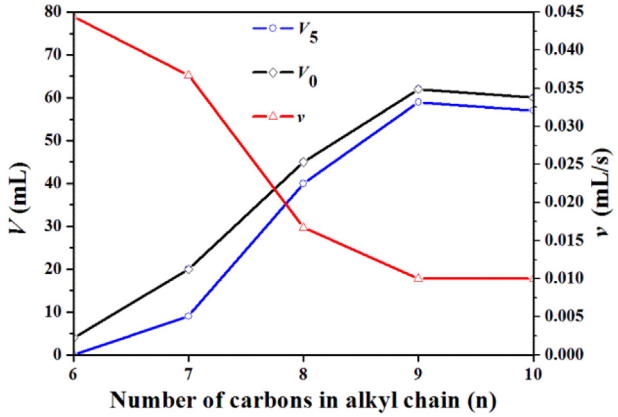

Fig. 5. Foam property of alkyl dioxyethyl α-*D*-xyloside (**5a-5e**).

4.5. Thermotropic liquid crystal property

The thermotropic liquid crystalline properties of the homologous series of alkyl dioxyethyl α-*D*-xyloside (**5a-5f**) with different alkyl chain lengths were investigated by the DSC and the POM, respectively.

Fig. 7 showed the DSC thermograms of decyl dioxyethyl α-*D*-xyloside (**5e**). Through the first cooling and the second heating processes at 5 °C·min^{-1}, there were two-phase transition peaks, the first phase transition was the melting point (solid → liquid crystalline), the second phase transition was the clearing point (liquid crystalline → liquid). Also, the peak area of the melting point was much larger than that of the clearing point, so the enthalpy required from anisotropic liquid crystal phase to the isotropic liquid phase was rather low. The DSC thermograms of dodecyl dioxyethyl α-*D*-xylosides (**5f**) were similar to decyl dioxyethyl α-*D*-xyloside (**5e**). For nonyl dioxyethyl α-*D*-xylosides (**5d**), its peak of the melting point did not appear, and the peak of the clearing point was not obvious, but its liquid crystalline property was observed by the POM and the clear point temperature was measured as 38.9 °C. The specific data were listed in Table 4.

In Table 4, for decyl dioxyethyl α-*D*-xyloside (**5e**), its melt point (*M*p) and clearing point (*C*p) were −19.2 °C and 30.5 °C, respectively. The length of the hydrophobic tail should directly have an impact on both of M_p and C_p [67]. Nevertheless, the phase transition temperature of alkyl dioxyethyl α-*D*-xyloside (**5f**) was found to have its data. Indeed, the stronger the intermolecular hydrogen bonds network and the weaker the van der Waals interactions, in general. Therefore, both interactions would just probably jointly determine the related phase transition temperature. Finally, nonyl dioxyethyl α-*D*-xyloside (**5d**) had only one transition peak due to its shorter hydrophobic alkyl chain [67,68].

The POM was used to investigate the thermotropic liquid crystal behavior. For alkyl dioxyethyl α-*D*-xylosides (**5a-5f**), their liquid crystalline properties began to appear in the heating process as its alkyl chain length n ≥ 9. From Fig. 8, alkyl dioxyethyl α-*D*-xylosides (**5d-5f**) were observed to have birefringent structures that were considered as the characteristic focal-conic fan schlieren textures below T_c during the cooling process [52,58]. Although **5f** had overall ambiguous focal-conic domains, whereas the focal-conic domains of **5e** were not big and their edges seemed very indistinct and even slight blurring to some content. In comparison, **5d** displayed the biggest and rather sharp focal-conic and fan-shaped schlieren domains, suggesting that such texture might be attributed as the lamellar phase and/or smectic phase which was similar to the stated texture in the previous studies [68,69]. The formed focal-conic and fan-shaped schlieren texture was characterized by hyperbolic and elliptical lines of optical discontinuity. Such ordered liquid crystal structures could perhaps be arranged in sequence by self-assembly and self-organizing formations due to the driving forces involving strong intermolecular hydrogen bonding network and weak intermolecular dispersion force. The phenomenon would perhaps lead to open a new channel for the research and development of liquid crystal light valve and light-addressable sugar-based material with favorable biodegradability and biocompatibility.

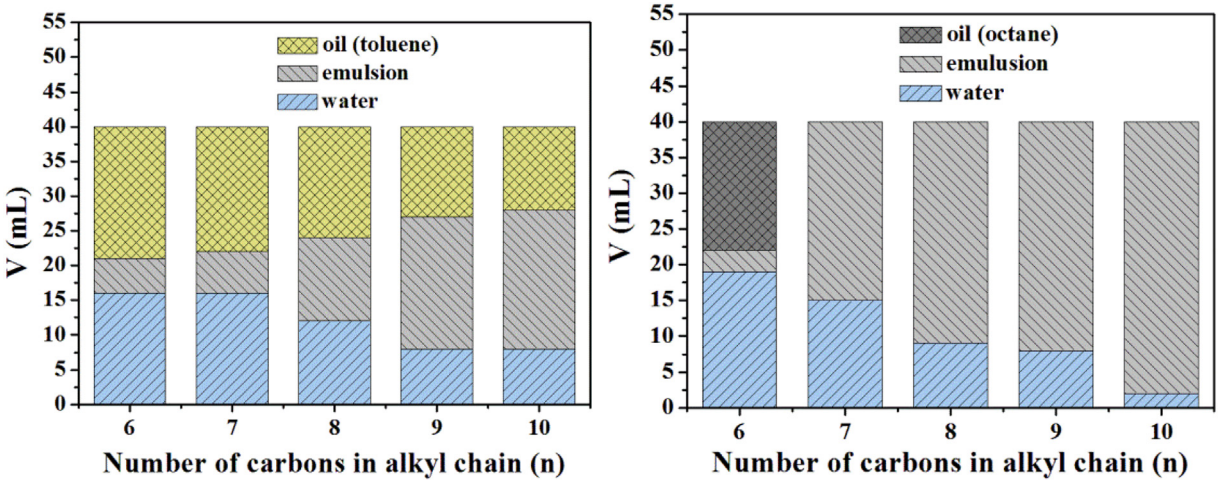

Fig. 6. Emulsifying property of alkyl dioxyethyl *α-D*-xylosides (**5a-5e**).

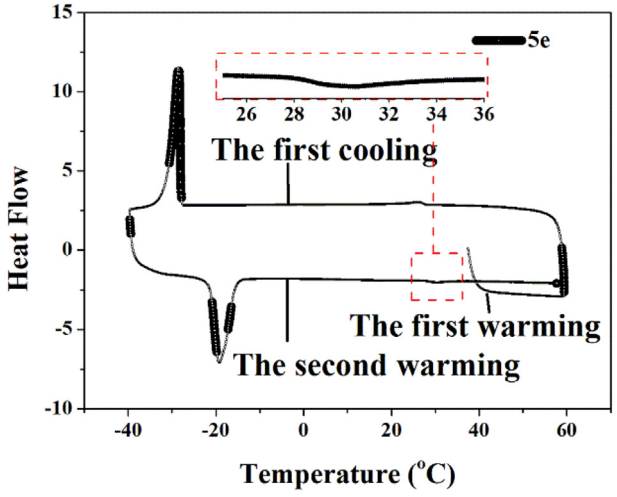

Fig. 7. Heat flow curve of decyl dioxyethyl *α-D*-xyloside (**5e**).

4.6. Hygroscopicity

The hygroscopicity of alkyl dioxyethyl *α-D*-xylosides (**5a-5f**) was determined with the relative humidity (*RH*) of 43% and 81%. The experimental results were shown in Fig. 9.

As seen in Fig. 9, their hygroscopicity weakened gradually with the extension of alkyl chain length. On the whole, the moisture absorption capacity of the samples was close to the highest level after 48 h. The hygroscopicity of **5a** (n = 6) had the same hygroscopic trend on the *RH* = 43% condition and on the *RH* = 81% condition. In the two *RH* systems, the hygroscopic ability of **5a** (n = 6) was the strongest. On the comparison, the hygroscopic ability of **5f** (n = 12) was the weakest.

Table 4
Thermotropic transition temperature and enthalpy under the second heating process with DSC scan.

Alkyl dioxyethyl *α-D*-xylosides	M_p (°C)	C_p (°C)	ΔT (°C)	ΔH_m (kJ·mol^{-1})	ΔH_c (kJ·mol^{-1})
5d (n = 9)	–	38.9	–	–	–
5e (n = 10)	−19.2	30.5	49.7	12.1	2.2×10^{-1}
5f (n = 12)	10.3	50.0	39.7	15.9	2.6×10^{-4}

Compared with the different *RH*, it could also be seen that the absorption rate of alkyl dioxyethyl *α-D*-xylosides for *RH* = 81% was greater than that for *RH* = 43%. Such *α-D*-xylosides had the hygroscopic properties, the main reason was that both of glycosyl group and dioxythylene fragment interacted with water by the intermolecular hydrogen bond network, so they could absorb efficiently the water from the environment. However, longer alkyl chain *α-D*-xylosides should have a low moisture absorption rate because of their smaller *HLB* number and bigger Log*P* value.

5. Conclusions

With *D*-xylose as the raw material, a series of 1,2-cis alkyl dioxyethyl *α-D*-xylosides (**5a-5f**) were stereoselectively synthesized via three-step reactions including the acetylation, the coupling reaction, and the deacetylation.

With the same *TPSA* value, their *HLB* number and water solubility decreased gradually with increasing alkyl chain length. Dodecyl dioxyethyl *α-D*-xyloside (**5f**) had not water solubility at all whereas hexyl dioxyethyl *α-D*-xyloside (**5a**) had strong water solubility. Also, compared with alkyl *α-D*-xyloside with the same alkyl chain length, alkyl dioxyethyl *α-D*-xylosides indeed improved the related water solubility due to the introduction of dioxyethylene fragment as the hydrophilic spacer to increase their *TPAS* value from 79.15 Å^2 (**7**) to 97.61 Å^2 (**5**). Their *CMC* values decreased with increasing the alkyl chain length. The *CMC* value of decyl dioxyethyl *α-D*-xyloside (**5e**) was as low as 9.21×10^{-5} mol·L^{-1}. Among them (**5a-5e**), octyl dioxyethyl *α-D*-xyloside (**5c**) had the lowest surface tension (27.25 mN·m^{-1}) at the *CMC*. Nonyl and decyl dioxyethyl *α-D*-xyloside (**5d** & **5e**) had good foaming power and foam stability. Decyl dioxyethyl *α-D*-xyloside (**5e**) had the strongest emulsifying property either in the toluene/water system or in the octane/water system. Moreover, glycosides (**5d**) had the most stylish focal-conic fan schlieren texture. The hygroscopicity of alkyl dioxyethyl *α-D*-xylosides (**5a-5f**) decreased gradually with increasing alkyl chain length although hexyl dioxyethyl *α-D*-xyloside (**5a**) possessed the strongest hygroscopicity.

In a word, such interesting and charming alkyl dioxyethyl *α-D*-xyloside indeed improved the water solubility and surface activity with the hygroscopicity and the thermotropic liquid crystalline behavior, In order to make full of the renewable and sustainable sugar resources and activate their practical application as novel sugar-based surfactants, it is suggested that a lot of the related technology [37], surface activity [70,71], synergistic effect, phase behavior [72], functional property [16,17,73], tolerance performance, toxicity [36], biodegradability, biocompatibility [29,33], structural modification [26,68], and

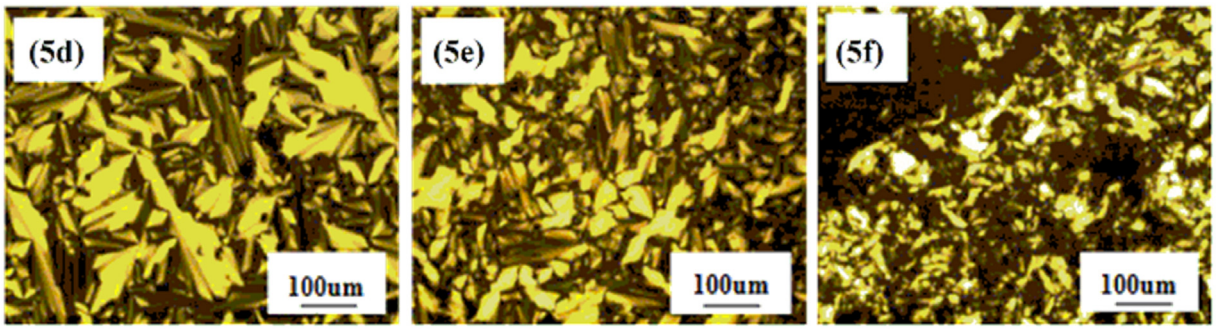

Fig. 8. Liquid crystal texture of alkyl dioxyethyl *α*-*D*-xylosides (**5d-5f**).

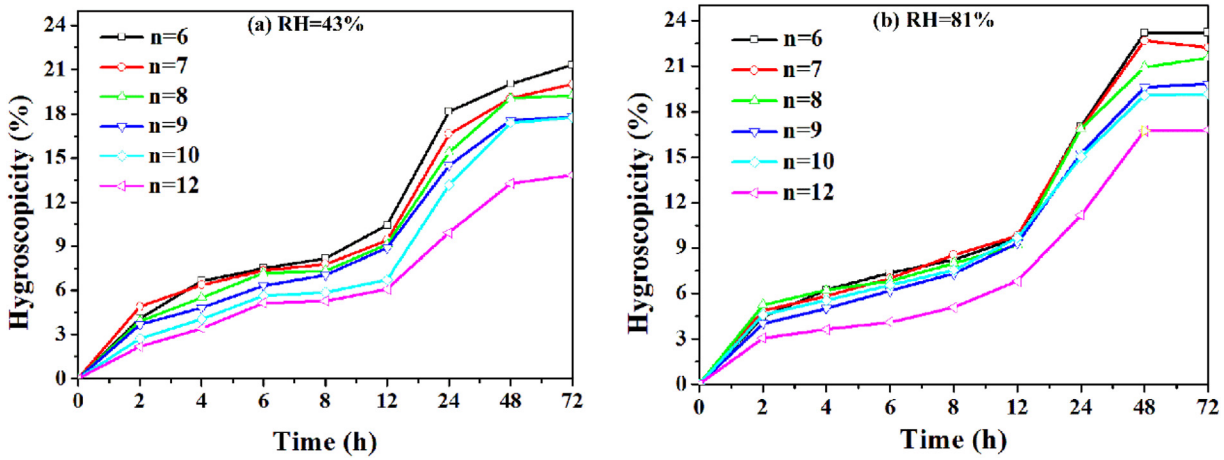

Fig. 9. Hygroscopicity of glycosides (**5a-5f**) (a) *RH* = 43%, (b) *RH* = 81%.

application [74,75] should be effectively investigated in the future in detail.

Declaration of competing interest

The authors declare that they have no known competing financial interests or personal relationships that could have appeared to influence the work reported in this paper.

Acknowledgments

This work was supported by the National Natural Science Foundation of China (grant numbers 21643010) and Hunan 2011 Collaborative Innovation Center of Chemical Engineering & Technology with Environmental Benignity and Effective Resource Utilization.

Appendix A. Supplementary data

Supplementary data to this article can be found online at https://doi.org/10.1016/j.molliq.2020.113770.

References

[1] Q. Zhang, Y. Li, Y. Song, J. Li, Z. Wang, J. Mol. Liq. 258 (2018) 34–39.
[2] Q. Deng, H. Li, H. Sun, Y. Sun, Y. Li, Colloid Surface B 141 (2016) 206–212.
[3] M.K. Matsson, B. Kronberg, P.M. Claesson, Langmuir 20 (2004) 4051–4058.
[4] M.K. Matsson, B. Kronberg, P.M. Claesson, Langmuir 21 (2005) 2766–2772.
[5] M.M. Abdulredha, S.A. Hussain, L.C. Abdullah, Arab. J. Chem. 13 (2020) 3403–3428.
[6] J.L. Schnoor, Environ. Sci. Technol. 42 (2008) 8615.
[7] A. Tullo, C&EN 98, 2020 12https://pubs.acs.org/doi/10.1021/cen-09811-buscon2.
[8] P. Ertl, B. Rohde, P. Selzer, J. Med. Chem. 43 (2000) 3714–3717.
[9] C. Adams, K.D. Collier, M.J. Pepsin, B. Schmidt, US20140193886 (2014).
[10] N. Ferlin, D. Grassi, C. Ojeda, M.J.L. Castro, A. Fernández-Cirelli, J. Kovensky, E. Grand, J. Surfactant Deterg. 15 (2012) 259–264.
[11] A.M.A. Hasan, M.E. Abdel-Raouf, Egypt. J. Pet. 27 (2018) 1043–1050.
[12] T. Zhao, Y. Chen, Y. Li, W. Pu, Y. He, J. Surfactant Deterg. 22 (2019) 821–832.
[13] B. Doshi, M. Sillanpää, S. Kalliola, Water Res. 135 (2018) 262–277.
[14] L.-H. Lin, H.-C. Chu, K.-M. Chen, S.-C. Chen, J. Surfactant Deterg. 22 (2019) 73–83.
[15] G.L. Visavale, R.K. Nair, S.S. Kamath, M.R. Sawant, B.N. Thorat, Dry. Technol. 25 (2007) 1369–1376.
[16] R. Hashim, A. Sugimura, H.-S. Nguan, M. Rahman, H. Zimmermann, J. Chem. Phys. 146 (2017), 084702. .
[17] M. Patrick, N.I. Zahid, M. Kriechbaum, R. Hashim, Liq. Crist. 45 (2018) 1970–1986.
[18] D. Terescenco, G. Savary, F. Clemenceau, E. Merat, B. Duchemin, M. Grisel, C. Picard, J. Mol. Liq. 253 (2018) 45–52.
[19] O. Misran, B.A. Timimi, T. Heidelberg, A. Sugimura, R. Hashim, J. Phys. Chem. B 117 (2013) 7335–7344.
[20] S.L. Guenic, L. Chaveriat, V. Lequart, N. Joly, P. Martin, J. Surfactant Deterg. 22 (2019) 5–21.
[21] F. Rong, D. Liu, D. Huang, Petrol. Sci. Technol. 36 (2018) 1613–1619.
[22] H.M. Feroz, H.Y. Kwon, J. Peng, H. Oh, B. Ferlez, C.S. Baker, J.H. Golbeck, G.C. Bazan, A.L. Zydney, M. Kumar, Analyst 143 (2018) 1378–1386.
[23] E. Nji, Y. Chatzikyriakidou, M. Landreh, D. Drew, Nat. Commun. 9 (2018) 4253.
[24] S. Lee, A. Mao, S. Bhattacharya, N. Robertson, J. Am. Chem. Soc. 138 (2016) 15425–15433.
[25] E. Reading, I. Liko, T.M. Allison, J.L.P. Benesch, A. Laganowsky, C.V. Robinson, Angew. Chem. 127 (2015) 4660–4664.
[26] X. Ge, S. Zhang, X. Chen, X. Liu, C. Qian, Green Chem. 21 (2019) 2771–2776.
[27] R. Khan, R. Irchhaiya, Int. J. Pharm. Bio Sci. 8 (2017) 106–116.
[28] S. Lucarini, L. Fagioli, R. Cavanagh, W. Liang, D.R. Perinelli, M. Campana, S. Stolnik, J.K.W. Lam, L. Casettari, A. Duranti, Pharmaceutics 10 (2018) 81.
[29] D.R. Perinelli, S. Lucarini, L. Fagioli, R. Campana, D. Vllasaliu, A. Duranti, L. Casettari, Eur. J. Pharm. Biopharm. 124 (2018) 55–62.
[30] K. Gavvala, R.K. Koninti, A. Sengupta, P. Hazra, Phys. Chem. Chem. Phys. 16 (2014) 14953–14960.
[31] N. Ahmad, R. Ramsch, M. Llinàs, C. Solans, R. Hashim, H.A. Tajuddin, Colloid Surface B 115 (2014) 267–274.
[32] W. Smułek1, E. Kaczorek1, Z. Hricovíniová, J. Surfactant Deterg. 20 (2017) 1269–1279.

[33] S.-A. Cho, J.-H. Han, S. An, K.H. Lee, J.-H. Park, H.K. Kim, T.R. Lee, Cutan. Ocul. Toxicol. 29 (2010) 50–56.
[34] R. Charoensapyanan, Y. Takahashi, S. Murakami, K. Ito, P. Rudeekulthamrong, J. Kaulpiboon, Appl. Biochem. Micro. 53 (2017) 410–420.
[35] S. Matsumura, K. Irnai, S. Yoshikawa, K. Kawada, T. Uchibori, J. Am. Oil Chem. Soc. 67 (1990) 996–1001.
[36] M.M. Fiume, B. Heldreth, W.F. Bergfeld, D.V. Belsito, R.A. Hill, C.D. Klaassen, D. Liebler, J.G. Marks Jr., R.C. Shank, T.J. Slaga, P.W. Snyder, F.A. Andersen, Int. J. Toxicol. 32 (2013) 22S–48S.
[37] M. Ochs, M. Muzard, R. Plantier-Royon, B. Estrined, C. Rémond, Green Chem. 13 (2011) 2380–2388.
[38] J. Angarska, C. Stubenrauch, E. Manev, Colloid Surface A 309 (2007) 189–197.
[39] A. Karam, K.D.O. Vigier, S. Marinkovic, B. Estrine, C. Oldani, F. Jérôme, ACS Catal. 7 (2017) 2990–2997.
[40] S. Watanabe, Carbohydr. Res. 343 (2008) 2325–2328.
[41] E.T. Maggio, Ther. Deliv. 4 (2013) 567–572.
[42] S. Ji, W. Shen, L. Chen, Y. Zhang, X. Wu, J. Mol. Liq. 242 (2017) 1169–1175.
[43] N. Kuang, G. Wu, L. Chen, S. Xia, Z. Li, G. Chen, X. Ye, J. Cent. South Univ. (Sci. Technol.) 47 (2016) 3323–3331.
[44] D.N. Moysés, V.C.B. Reis, J.R.M. de Almeida, L.M.P. de Moraes, F.A.G. Torres, Int. J. Mol. Sci. 17 (2016) 207.
[45] J. Rowley, S.R. Decker, W. Michener, S. Black, 3 Biotech 3 (2013) 433–438.
[46] K.L. Ong, C. Li, X. Li, Y. Zhang, J. Xu, C.S.K. Lin, Biochem. Eng. J. 148 (2019) 108–115.
[47] R.K. Mishra, V.B. Kumar, A. Victor, I.N. Pulidindi, A. Gedanken, Ultrason. Sonochem. 56 (2019) 55–62.
[48] G.G. Sivets, F. Amblard, R.F. Schinazi, Tetrahedron 75 (2019) 2037–2046.
[49] H. Cui, J. Yu, S. Xia, E. Duhoranimana, Q. Huang, X. Zhang, Food Chem. 271 (2019) 47–53.
[50] Y. Feng, M. Yao, Y. Wang, M. Ding, J. Zha, W. Xiao, Y. Yuana, Biotechnol. Adv. 41 (2020) 107538.
[51] B. Helferich, E. Schmitz-Hillebrecht, Berichte der deutschen chemischen Gesellschaft (A and B series) 66 (1933) 378–383.
[52] S. Ji, W. Shen, L. Chen, Y. Zhang, X. Wu, Y. Fan, F. Fu, G. Chen, Colloid Surface A 564 (2019) 59–68.
[53] X. Wu, L. Chen, Y. Fan, F. Fu, J. Li, J. Zhang, J. Agric. Food Chem. 67 (2019) 10361–10372.
[54] R.C. Pasquali, M.P. Taurozzi, C. Bregni, Int. J. Pharm. 356 (2008) 44–51.
[55] Z. Li, G. Chen, L. Chen, Y. Zhang, Z. Dai, J. Surfact. Deterg. 22 (2019) 731–742.
[56] P. Szumała, A. Mówińska, J. Surfactant Deterg. 19 (2016) 437–445.
[57] T. Yoshimura, A. Sakato, K. Tsuchiya, T. Ohkubo, H. Sakai, M. Abe, K. Esumi, J. Colloid Interf. Sci. 308 (2007) 466–473.
[58] X. Wu, L. Chen, F. Fu, Y. Fan, Z. Luo, J. Mol. Liq. 276 (2019) 282–289.
[59] L. Chen, F. Kong, Carbohydr. Res. 337 (2002) 2335–2341.
[60] B.J. Boyd, C.J. Drummond, I. Krodkiewska, F. Grieser, Langmuir 16 (2000) 7359–7367.
[61] C. Serafim, I. Ferreira, P. Rijo, L. Pinheiro, C. Faustino, A. Calado, L. Garcia-Rio, Int. J. Pharm. 497 (2016) 23–35.
[62] T. Yoshimura, S. Umezama, A. Fujino, K. Torigoe, K. Sakai, H. Sakai, M. Abe, K. Esumi, J. Oleo Sci. 62 (2013) 353–362.
[63] A. Nesterenko, A. Drelich, H. Lu, D. Clausse, I. Pezron, Colloid Surfaces A 457 (2014) 49–57.
[64] B. Niraula, T.C. King, T.K. Chun, M. Misran, Colloid Surface A 251 (2004) 117–132.
[65] J. Huo, X. Liu, J. Niu, J. Surfactant Deterg. 18 (2015) 523–528.
[66] E. Ruckenstein, Langmuir 12 (1996) 6351–6353.
[67] D. Häntzschel, J. Schulte, S. Enders, K. Quitzsch, Phys. Chem. Chem. Phys. 1 (1999) 895–904.
[68] J.W. Goodby, V. Görtz, S.J. Cowling, G. Mackenzie, P. Martin, D. Plusquellec, T. Benvegnu, P. Boullanger, D. Lafont, Y. Queneau, S. Chambert, J. Fitremann, Chem. Soc. Rev. 36 (2007) 1971–2032.
[69] G. Milkereit, M. Morr, J. Thiema, V. Vill, Chem. Phys. Lipids 127 (2004) 47–63.
[70] Y. Fan, F. Fu, L. Chen, J. Li, J. Zhang, J. Agric. Food Chem. 68 (2020) 2684–2695.
[71] T. Gaudin, H. Lu, G. Fayet, A. Berthauld-Drelich, P. Rotureau, G. Pourceau, A. Wadouachi, E.V. Hecke, A. Nesterenko, I. Pezron, Adv. Colloid Interfac 270 (2019) 87–100.
[72] N. Rahim, N. Ahmat, J.S. Norrizah, N.F.K. Aripin, H.A.A. Hamid, A. Saleh, Mater. Today: Proceedings 5 (2018) S180–S185.
[73] A. Martinez-Felipe, T.S. Velayutham, N.F.K. Aripin, M. Yusoff, E. Farquharson, R. Hashim, Liq. Crist. (2020)https://doi.org/10.1080/02678292.2020.1750719.
[74] S. Berkley, Science 367 (2020) 1407.
[75] T. Mizumura, K. Kondo, M. Kurita, Y. Kofuku, M. Natsume, S. Imai, Y. Shiraishi, T. Ueda, I. Shimada, Sci. Adv. 6 (2020) eaay8544.